Communication

Ultrafast Deactivation Channel for Thymine Dimerization

Martial Boggio-Pasqua, Gerrit Groenhof, Lars V. Schfer, Helmut Grubmller, and Michael A. Robb

J. Am. Chem. Soc., **2007**, 129 (36), 10996-10997• DOI: 10.1021/ja073628j • Publication Date (Web): 16 August 2007

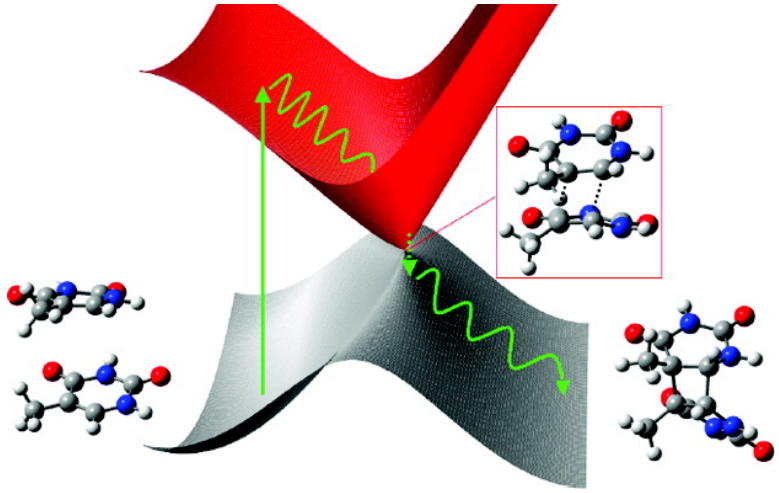

J|A|C|S
COMMUNICATIONS

Published on Web 08/16/2007

Ultrafast Deactivation Channel for Thymine Dimerization

Martial Boggio-Pasqua,[†] Gerrit Groenhof,[‡] Lars V. Schäfer,[‡] Helmut Grubmüller,[‡] and Michael A. Robb*,[†]

Department of Chemistry, Imperial College London, London SW7 2AZ, United Kingdom, and Department of Theoretical and Computational Biophysics, Max-Planck-Institute for Biophysical Chemistry, Am Fassberg 11, 37077 Göttingen, Germany

Received May 21, 2007; E-mail: mike.robb@imperial.ac.uk

Intrastrand thymine dimerization (Figure 1) is recognized as the most common process leading to DNA damage under ultraviolet (UV) irradiation.[1] The formation of thymine dimers has potentially important physiological consequences. This mutagenic photoproduct can disrupt the function of DNA and thereby trigger complex biological responses, including apoptosis, immune suppression, and carcinogenesis.[2−4]

A very recent study[5] based on femtosecond time-resolved infrared spectroscopy showed that thymine dimers are fully formed around 1 ps after UV excitation. The authors concluded that this ultrafast photolesion rate points to an excited-state reaction that is nearly barrierless for bases that are properly oriented at the instant of light absorption. It was suggested that the low quantum yield of this photoreaction results from infrequent conformational states in the unexcited system. However, this study did not provide a mechanistic picture of the photoactivated thymine dimerization process.

In this study, we have identified by quantum chemical calculations the photochemical pathway leading to the formation of the thymine dimer in the gas phase and characterized the funnel required for this ultrafast process. Our results show that, while the thermally induced [2 + 2] cycloaddition of two stacked thymines proceeds through a highly activated stepwise mechanism on the ground state, the photoreaction occurs via a barrierless concerted mechanism on a singlet excited state. The latter mechanism is nonadiabatic and takes place through an S_0/S_1 conical intersection (CI), which is the funnel for ultrafast nonradiative decay leading to the thymine dimer (see Figure 1b).

Time-dependent density functional theory studies[6,7] showed a narrowing of the ground state (S_0) and first singlet excited state (S_1) energy gap along the thermally induced [2 + 2] cycloaddition reaction pathway. The first triplet state was also shown to possibly play a role in the dimerization, although at a slower rate than on the singlet excited state. However, this study did not consider the excited reaction path, and the channel for nonradiative decay to the ground state leading to the photoproduct was not identified.

Here, the complete active space self-consistent field (CASSCF) method was used to calculate the S_0 and S_1 electronic states of the two thymine molecules. The choice of the orbital active space and results obtained at the second-order perturbation theory (CASPT2) are given in the Supporting Information (Figures S1 and S2). Twelve electrons were distributed among twelve orbitals. The 6-31G*[8] and correlation consistent cc-pVDZ[9] basis sets were used for CASSCF and CASPT2, respectively. Geometry optimizations were performed in the full nuclear configuration space. However, since unconstrained geometry optimization of two stacked thymines yields a structure with an orientation unlikely to occur in the DNA strand due to steric tensions, we also reoptimized the reactant

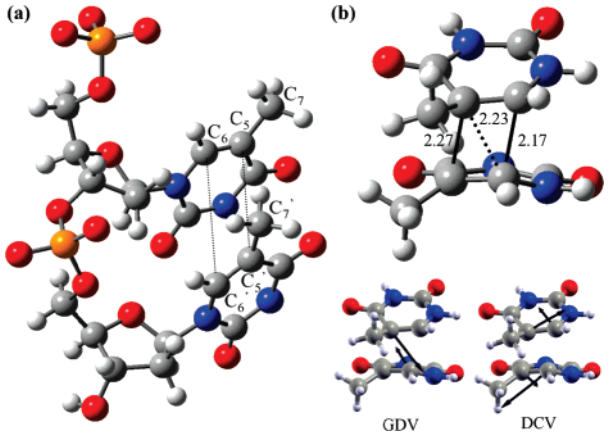

Figure 1. (a) Stacked thymines in DNA. (b) Structure of the S_0/S_1 conical intersection, S_0/S_1-*CI*. Gradient difference (GDV) and derivative coupling (DCV) vectors forming the branching space. Interatomic distances are given in Å.

complex with the same constraints as used in refs 6 and 7 ($C_5-C_5' = 4.18$ Å, $C_6-C_6' = 4.46$ Å, and $C_7-C_5-C_5'-C_7' = 35.3°$ as in B-DNA dodecamer[10]). Optimized structures were fully characterized by analytical frequency calculation at the CASSCF level using a reduced active space. State-averaged orbitals were used for the CI optimization, and orbital rotation derivative correction (which is usually small) to the gradient was neglected. Single-point energy calculations were carried out at linearly interpolated structures between the Franck−Condon (FC) geometries and the CI to characterize the excited-state reaction pathway. All CASSCF and CASPT2 calculations were performed using Gaussian[11] and MOLPRO,[12] respectively.

The ground-state potential energy profile for the thermal [2 + 2] cycloaddition of two stacked thymines is shown in Figure 2. This process takes place through a highly activated stepwise mechanism, as expected from Woodward−Hoffmann rule[13] for a "forbidden" thermal reaction. The first transition state, S_0-*TS1*, connects the stacked thymine minimum, S_0-*open*, to the intermediate biradical minimum, S_0-*biradical*, with a barrier height of 61 kcal/mol. This barrier is relative to the constrained stacked thymines. Note that the unconstrained S_0-*open* minimum lies only 0.26 kcal/mol below in energy (Figure S3 in Supporting Information). The transition vector of S_0-*TS1* corresponds to the C_6-C_6' bond stretching (Figure S4 in Supporting Information). The biradical intermediate, S_0-*biradical*, is found only 1.2 kcal/mol below S_0-*TS1*. This biradical structure then proceeds to the thymine dimer via a second transition state, S_0-*TS2*, lying 3.3 kcal/mol above the biradical. Its transition vector involves the second C−C bond formation of the cyclization process, that is, the C_5-C_5' bond stretching (Figure S5 in Supporting Information). The thymine dimer minimum, S_0-*closed*, is found 19 kcal/mol above S_0-*open*.

[†] Imperial College London.
[‡] Max-Planck-Institute.

10.1021/ja073628j CCC: $37.00

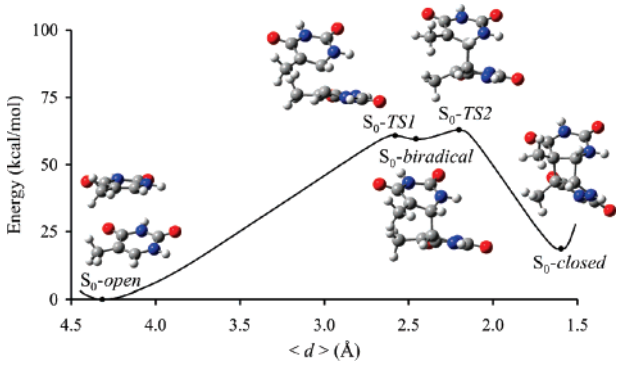

Figure 2. CASSCF ground-state potential energy profile for the thermally induced [2 + 2] cycloaddition of two stacked thymines. <*d*> represents the average distance between the two forming C−C bonds.

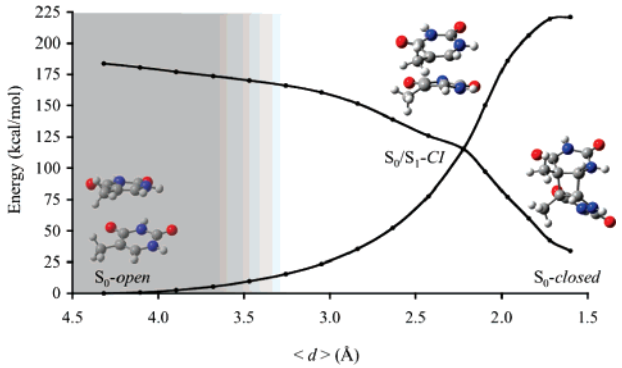

Figure 3. CASSCF singlet excited-state potential energy profile for the photochemical [2 + 2] cycloaddition of two stacked thymines. The shaded area indicates the region expected to be altered by the DNA environment. <*d*> represents the average distance between the two forming C−C bonds.

This potential energy profile clearly shows that the thymine dimerization cannot take place on the ground state.

Unlike the ground-state reaction pathway, the excited-state photochemical [2 + 2] cycloaddition takes place through a concerted mechanism (Figure 3). This barrierless process leads to a low-lying conical intersection, S_0/S_1-*CI*, where ultrafast nonradiative decay to the ground state is extremely efficient. Such a nonadiabatic pathway has already been found in the ethylene−ethylene photochemical cycloaddition.[14]

The structure of the CI is shown in Figure 1b. The two branching space coordinates that lift the degeneracy at first order are also shown in this figure. They both involve motion in the $C_5-C_6-C_6'-C_5'$ ring. The "peaked" topology of the CI suggests that upon decay to the ground state at S_0/S_1-*CI* the system can either evolve to the photoproduct S_0-*closed* or reverse back to the original reactant S_0-*open*. Inclusion of dynamic electron correlation at the CASPT2 level confirms the geometry and surface topology of the CI (Figure S2 in Supporting Information). Note that the FC region of the excited-state potential energy surface in the gas phase (shaded area in Figure 3) may not be relevant for the thymine dimerization in DNA because the DNA environment and dynamic electron correlation effects are expected to alter this part of the energy profile and the order of the states. Furthermore, initial population of other electronic states will lead to other decay channels (see discussion below).

In conclusion, we have identified and characterized the excited-state reaction pathway leading to the formation of the potentially mutagenic thymine dimer in the gas phase. Our results show that the photodimerization can proceed via a concerted mechanism on a singlet excited state, which leads to an S_0/S_1 conical intersection. Schreier et al.[5] suggest that there is a strong link between conformation before light absorption and photodamage. They suggest that the low quantum yield for thymine dimerization results from rare conformational states in the unexcited DNA strand. On the basis of the present study and the experimental observations, we speculate that photoexcitation within the DNA will lead to a spontaneous concerted [2 + 2] cycloaddition if the two neighboring thymines are at a configuration near the S_0/S_1-*CI* geometry. The low dimerization quantum yield suggests that such configurations are infrequent in the unexcited DNA. Furthermore, excitation at highly populated B-DNA configurations, that is, further away from the CI, may not lead to photodimerization, as alternative deactivation pathways, such as interstrand proton transfer[15a] or out-of-plane deformation of a single thymine,[15b] could be more easily accessible. In a follow-up study, we will address these competing photochemical processes in the DNA environment by means of QM/MM excited-state molecular dynamics simulations.[16]

Acknowledgment. This work has been supported by EPSRC UK (grant GR/S94704/01). Support from the EU Nanomot project (grant 29084) is thankfully acknowledged.

Supporting Information Available: Cartesian coordinates and absolute energies for optimized CASSCF structures. Figure S1 for choice of active orbitals and Figure S2 for CASPT2 results. Figure S3 for free and constrained stacked thymines. Figures S4 and S5 for S_0-*TS1* and S_0-*TS2* transition vectors. Complete refs 11 and 12. This material is available free of charge via the Internet at http://pubs.acs.org.

References

(1) Cadet, J.; Vigny, P. In *Bioorganic Photochemistry*; Morrison, H., Ed.; Wiley: New York, 1990; pp 1−272.
(2) Taylor, J. S. *Acc. Chem. Res.* **1994**, *27*, 76.
(3) Vink, A. A.; Roza, L. *J. Photochem. Photobiol. B* **2001**, *65*, 101.
(4) Melnikova, V. O.; Ananthaswamy, H. N. *Mutat. Res.* **2005**, *571*, 91.
(5) Schreier, W. J.; Schrader, T. E.; Koller, F. O.; Gilch, P.; Crespo-Hernández, C. E.; Swaminathan, V. N.; Carell, T.; Zinth, W.; Kohler, B. *Science* **2007**, *315*, 625−629.
(6) Durbeej, B.; Eriksson, L. A. *J. Photochem. Photobiol. A* **2002**, *151*, 95−101.
(7) Zhang, R. B.; Eriksson, L. A. *J. Phys. Chem. B* **2006**, *110*, 7556−7562.
(8) (a) Hehre, W. J.; Ditchfield, R.; Pople, J. A. *J. Chem. Phys.* **1972**, *56*, 2257. (b) Hariharan, P. C.; Pople, J. A. *Theor. Chim. Acta* **1973**, *28*, 213.
(9) Dunning, T. H. *J. Chem. Phys.* **1989**, *90*, 1007−1023.
(10) Shui, X.; McFail-Isom, L.; Hu, G. G.; Williams, L. D. *Biochemistry* **1998**, *37*, 8341−8355.
(11) Frisch, M. J.; et al. *Gaussian Development Version*, revision B.07; Gaussian, Inc.: Pittsburgh, PA, 2003.
(12) Werner, H.-J.; et al. *MOLPRO*, version 2006.1.
(13) Woodward, R. B.; Hoffman, R. In *The Conservation of Orbital Symmetry*; Verlag Chemie: Weinheim, Germany, 1970.
(14) (a) Bernardi, F.; De, S.; Olivucci, M.; Robb, M. A. *J. Am. Chem. Soc.* **1990**, *112*, 1737−1744. (b) Bernardi, F.; Olivucci, M.; Robb, M. A. *Acc. Chem. Res.* **1990**, *23*, 405−412. (c) Celani, P.; Robb, M.A.; Garavelli, M.; Bernardi, F.; Olivucci, M. *Chem. Phys. Lett.* **1995**, *243*, 1−8.
(15) (a) Perun, S.; Sobolewski, A. L.; Domcke, W. *J. Phys. Chem. A* **2006**, *110*, 9031−9038. (b) Perun, S.; Sobolewski, A. L.; Domcke, W. *J. Phys. Chem. A* **2006**, *110*, 13238−13244.
(16) Groenhof, G.; Bouxin-Cademartory, M.; Hess, B.; de Visser, S. P.; Berendsen, H. J. C.; Olivucci, M.; Mark, A. E.; Robb, M. A. *J. Am. Chem. Soc.* **2004**, *126*, 4228−4232.

JA073628J